

15C.1 – THE OVERLAND REINTENSIFICATION OF NORTH ATLANTIC TROPICAL CYCLONE ERIN (2007): PHYSICAL AND DYNAMICAL CHARACTERISTICS

Clark Evans

NCAR Earth System Laboratory, Boulder, CO
evans@ucar.edu

Russ S. Schumacher
Texas A&M University
Dept. of Atmospheric Sciences

Thomas J. Galarneau
State University of New York, Univ. at Albany
Dept. of Earth and Atmospheric Sciences

1. Introduction

During the early morning hours of 19 August 2007, nearly three days after making landfall as a tropical depression on the central Texas coastline, the remnant circulation associated with North Atlantic Tropical Cyclone (TC) Erin dramatically re-intensified over western Oklahoma. Associated with this reintensification were a pressure fall of 12 hPa (1007 to 995 hPa) and surface wind speed acceleration of 30 kt (20 to 50 kt) between 1800 UTC 18 August 2007 and 0600 UTC 19 August 2007 (Knabb 2008). The reintensification of the remnant TC also brought about the development of an eye-like feature, as evidenced by WSR88-D Doppler radar imagery over west-central Oklahoma early on the 19th of August (Figure 1). The works of Knabb (2008) and Brennan et al. (2009) provide further insight into the entire life cycle of TC Erin's evolution while the work of Arndt et al. (2009) details observations during the reintensification period from the Oklahoma Mesonet network of weather stations.

Arndt et al. (2009) note that the inland reintensification of TC Erin is not the only case of a remnant TC bringing tropical storm-force winds to Oklahoma; five other TCs in the historical database, all prior to 1965, also brought such conditions to the state. What makes TC Erin unique amongst these cases, however, is that it was a weak TC at landfall and did not maintain tropical storm-force winds until reaching Oklahoma. Furthermore, they note that TC Erin is not the only example of a remnant TC that re-intensified over land not as a result of it transforming into an extratropical cyclone by means of the

extratropical transition process (Jones et al. 2003); at least two other cyclones, TCs David of 1979 and Danny of 1997, also re-intensified over land – specifically, in the northeastern United States – well after making landfall. Apart from the geographical region and characteristics of reintensification, what makes TC Erin unique from these cases is that it achieved a maximum intensity over land well in excess of that reached over water (Arndt et al. 2009).

Despite the inherently unique nature to TC Erin's reintensification, previous works provide some insight into factors potentially contributing to the reintensification process. Arndt et al. (2009) synthesized the findings of Bosart and Lackmann (1995) and Bassill and Morgan (2006) as relating to the overland reintensifications of TCs David (1979) and Danny (1997), respectively, and noted that both reintensifications occurred in moist, conditionally unstable atmospheres with weak extratropical forcing, no surface baroclinic zone, and strong diabatic heating resulting from deep convection. Tuleya (1994) and Shen et al. (2002) described wet, oceanic-like land conditions as favorable for TC maintenance or intensification over land. Chang et al. (2009) note similar moist surface conditions aiding the maintenance of monsoon depressions after landfall in India. Additionally, Emanuel et al. (2008) posed that warm-core vortices can re-intensify over land in an environment of high latent heat fluxes caused by the wetting of hot, sandy soils by rainfall ahead of the vortex. This mode of reintensification draws heavily of the surface latent heat flux theories of Emanuel (1986) and later works.

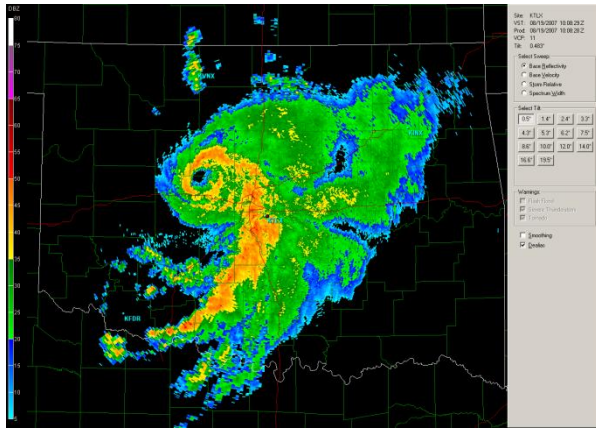


Figure 1: Level II WSR88-D 0.5° tilt base reflectivity scan of TC Erin (2007) at 10:08:29 UTC 19 August from the Oklahoma City/Norman, OK (KTLX) radar.

With respect to the TC Erin (2007) case in particular, Emanuel (2008) suggested that strong heating of soils containing significantly above average soil moisture due to above average rainfall in March through July 2007 (as noted by Arndt et al. 2009) led to conditions allowing for a tropical-like reintensification of the remnant TC Erin vortex on the morning of 19 August 2007. Brennan et al. (2009) and Knabb (2008) discuss the importance of weak extratropical forcing provided by a shortwave trough passing to the north of the remnant Erin vortex to the reintensification process. Finally, Arndt et al. (2009) note the importance of latent heat release associated with deep convection triggered in the vicinity of the remnant vortex. This convection, they pose, is triggered by lift associated with the aforementioned shortwave trough in an uncharacteristically unstable (for August in Oklahoma) thermodynamic environment. Despite these hypotheses, there remains no clear agreement as to the mechanisms that led to the reintensification of TC Erin (2007) over Oklahoma on 19 August 2007.

From the available observations and results from previous works, we pose the hypothesis that two factors were necessary conditions influencing the reintensification of the TC Erin vortex. First, convergence and lift associated with the cyclone-influenced, diurnally-driven nocturnal lower tropospheric jet across the southern Plains enhanced

by the movement of the remnant vortex into the axis of the jet promoted the development of convection to the south and east of the remnant vortex. Secondly, a moist, unstable boundary layer environment maintained in part by the wetting of soils across southern and central Texas by rains associated with the vortex on 16-17 August promoted more vigorous convective updrafts and thus greater latent heat release and transport aloft, leading to the intensification of the vortex. While a weak reintensification may occur with only one mechanism in place, we pose that the dramatic reintensification observed with TC Erin requires both contributions. In this work, we set out to test this hypothesis – as well as those presented by the aforementioned works – through the use of an ensemble of convection-permitting 4 km Advanced Research WRF (WRF-ARW; Skamarock et al. 2008) simulations of the evolution of the remnant TC Erin vortex over the Southern Plains. The formulation of this ensemble and the overall study methodology are presented in Section 2. Results from this ensemble, including a physical and dynamical discussion of the findings on the synoptic-scale to the meso- α scale, are presented in Section 3. A discussion of these results and concluding remarks are presented in Section 4 and are followed by acknowledgments and references.

2. Methodology

To study the reintensification period of TC Erin (2007), we employ an ensemble of convection-permitting WRF-ARW simulations encompassing the time period between 0000 UTC 18 August 2007-1800 UTC 19 August 2007. The control simulation (CONTROL) is conducted at a horizontal grid spacing of 4 km over a 560x536x30 domain centered over west-central Arkansas. Model initial and boundary conditions are provided by 1° NCEP GFS operational analyses. The Yonsei University planetary boundary layer (PBL) and Lin et al. microphysical schemes are employed within this simulation. Note that the evolution of the control simulation is found to be relatively insensitive to the selection of PBL and microphysical schemes (not shown). The NOAA land-surface model is used to simulate interactions

between the PBL and the surface. The control simulation exhibits slight slow and weak biases with the simulated cyclone as compared to reality (not shown) but does a reasonably good job in simulating the observed structures associated with the reintensifying vortex, including the north-south oriented rain band to the east of the vortex and the eye-like feature that developed early on 19 August 2007 (c.f. Figure 2 to Figure 1).

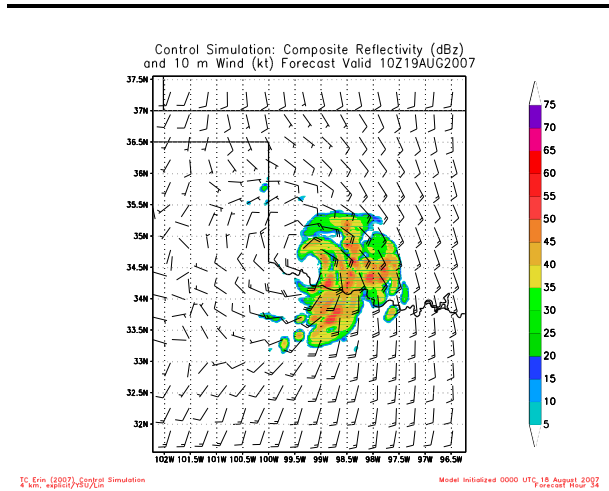


Figure 2: Composite reflectivity (shaded; dBz) and 10 m wind speeds (barbs; kt) at 1000 UTC 19 August 2007 from the 4 km WRF-ARW control simulation of TC Erin.

The ensemble of simulations conducted as a part of this work is primarily comprised of the control simulation described above and six soil condition perturbation members for a total of seven members. These simulations are designed to elucidate the role of the vortex and the near-surface thermodynamic environment in the reintensification process. In each case, apart from what is changed within the soil conditions or the land-surface model, the simulation formulation is identical to that described for the control simulation above.

The six soil condition perturbation members are broken down as follows. The first ensemble member (DRY) utilizes completely dry soil conditions over the simulation domain. The second ensemble member (AVG) is obtained using 1979-2006 average August soil moisture conditions as obtained from the

North American Regional Reanalysis (NARR). The third ensemble member (LOWMOIST) is obtained by subtracting three standard deviations from the 1979-2006 average August soil moisture conditions noted with AVG above. The fourth ensemble member (LOWTEMP) is obtained similarly to LOWMOIST, except by subtracting three standard deviations from the 1979-2006 average August NARR soil temperature conditions. The fifth ensemble member (LOWT+M) utilizes both the reduced soil temperature and soil moisture datasets described with LOWTEMP and LOWMOIST above. Finally, the sixth ensemble member (MIX) utilizes August 2007 soil moisture conditions along and within 1-2° of the simulated cyclone’s track and dry soil conditions elsewhere. Care is taken to ensure consistency among the soil temperature and moisture input data sources and the NOAA land-surface model employed within the WRF-ARW simulations conducted here (Koster et al. 2009). Comparisons of the observed August 2007 soil moisture conditions to those employed in simulations AVG, LOWMOIST, and MIX are depicted in Figures 3 and 4. Much of the results presented in this work are comprised from the results of the control simulation and these six ensemble members.

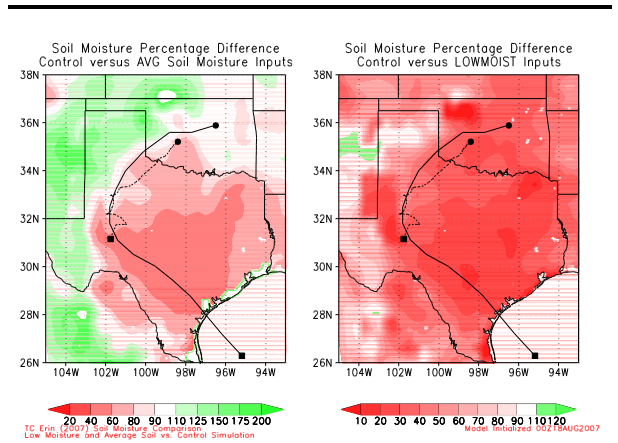


Figure 3: Percentage differences (red = moister in the control simulation) between the control and AVG soil moisture inputs (left) and the control and LOWMOIST soil moisture inputs (right). The observed (solid) and control run simulated (dashed) tracks of TC Erin are depicted by the black lines in each panel.

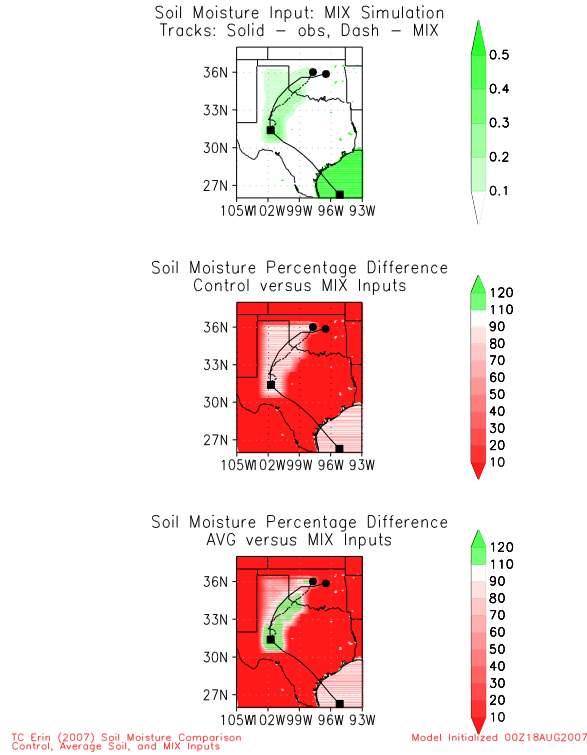


Figure 4: (top) Fractional soil moisture inputs used for the MIX ensemble member. (middle) As in Figure 3, except for the control and the MIX soil moisture inputs. (bottom) As in Figure 3, except for the AVG and MIX soil moisture inputs. In this panel, red signifies moister soil conditions in the AVG simulation.

To aid in determining the role of latent heat fluxes in the vicinity of the vortex to the reintensification process, seven land-surface model perturbation simulations are conducted. Four of these simulations are obtained by shutting off the precipitation feedback mechanism within the NOAH land-surface model, effectively causing latent heat fluxes to be zero in areas of active precipitation starting at various times within the model simulation. The remaining three simulations are obtained by shutting off latent heat fluxes altogether throughout the model simulation domain starting at various times within the model simulation. The results from these seven simulations are used primarily to refine the conclusions drawn from the main ensemble of seven simulations.

3. Results

3.1 Soil condition perturbation simulation results

Amongst the seven primary ensemble member simulations, two were able to reproduce a reintensification similar to that observed with TC Erin (2007) while five were unable to do so. The control simulation and member LOWTEMP were the two members that were able to reproduce the reintensification, both showing pressure falls on the order of 8 hPa/12 hr on the morning of 19 August 2007 (black line in Figure 5). The other five members – DRY, AVG, LOWMOIST, LOWT+M, and MIX – were unable to do so, though weak pressure falls of 1-3 hPa/12 hr were observed in each case (green line in Figure 5). We hypothesize that the weak pressure falls associated with these three cases are on the order of those that are observed due to the diurnal cycle of precipitation observed with remnant TC circulations overland (potentially by the mechanism described by Shen et al. 2002) and thus constitute the background signal within the observations of the reintensification process.

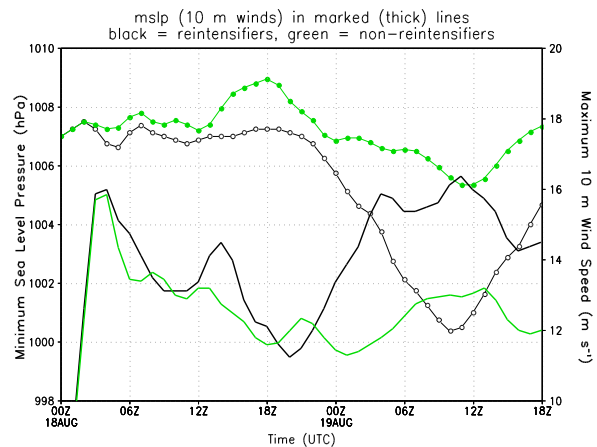


Figure 5: Evolution of the mean sea level pressure (hPa; marked lines) and 10 m maximum wind speed ($m s^{-1}$, solid lines) between 0000 UTC 18 August 2007 and 1800 UTC 19 August 2007 in the reintensifying (black lines) and non-reintensifying (green lines) composites.

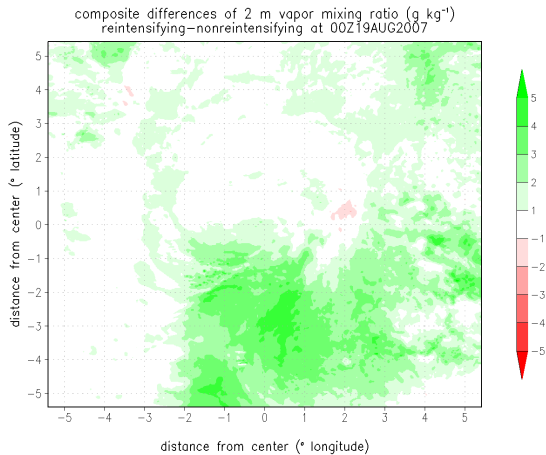


Figure 6: Cyclone-centered reintensifying minus non-reintensifying composite difference in the 2 m vapor mixing ratio field (g kg^{-1}) at 0000 UTC 19 August 2007.

We now turn to understanding how these differing soil conditions modulate the environment surrounding the simulated cyclone. To do so, storm-centered composites of model simulated thermodynamic fields are created. Figure 6 depicts the composite difference, defined here as the reintensifying composite minus the non-reintensifying composite, in the 2 m vapor mixing ratio at 0000 UTC 19 August 2007 as the reintensification process began. A significantly moister near-surface environment is observed in the cases where the simulated cyclone reintensified as compared to those in which it did not with mixing ratio differences on the order of $3\text{--}5 \text{ g kg}^{-1}$, or 30–40% of the total mixing ratio value (not shown). A similar evolution is noted at 850 hPa in the composite difference of equivalent potential temperature (Figure 7), where a composite difference of 3–4 K (354 K in the reintensifying simulations, 350–352 K in the non-reintensifying simulations) is observed. A warmer, moister boundary layer profile manifests itself in greater surface-based convectively available potential energy (SBCAPE) in the reintensifying cases as compared to the non-reintensifying cases (Figure 8). Differences between 200 J kg^{-1} and 1000 J kg^{-1} are observed between these two composites, with the simulations featuring

greater soil moisture content also exhibiting greater environment SBCAPE. Note again that these differences are concentrated to the south and east of the simulated vortex. Boundary layer streamline analyses from the cases presented in Figure 8 suggest that these differences are concentrated along the axis of the developing lower tropospheric jet as well as along a convergence axis situated south and east of the cyclone along which the primary rain band evolves (not shown). In all, the thermodynamic environment in the regions where convection develops within each of the simulations is more favorable for deep convection in the reintensifying as compared to the non-reintensifying cases.

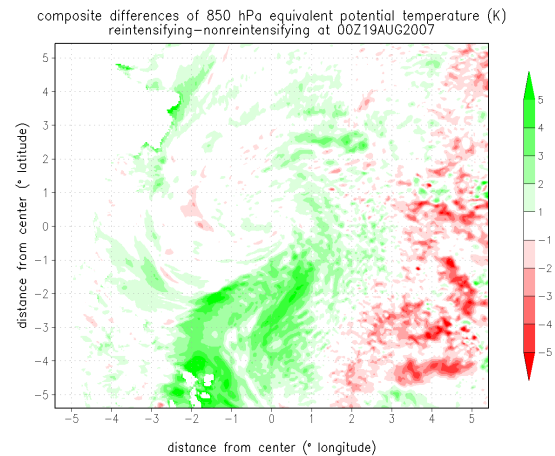


Figure 7: As in Figure 6, except for 850 hPa equivalent potential temperature (K).

Having highlighted the differences between the basic vortex evolution and the environmental thermodynamic characteristics associated with the reintensifying and non-reintensifying ensemble members, we now turn to highlighting the differences in the simulated latent heat flux fields both underneath and in the vicinity of the simulated cyclone. The composite latent heat flux difference field is shown in Figure 9 at two times: 0000 UTC 19 August 2007, as the reintensification process was beginning, and 0600 UTC 19 August 2007, as the reintensification process was ongoing. At the start of the reintensification process (Figure 9a), differences on the order of $50\text{--}75 \text{ W m}^{-2}$ are noted both in the

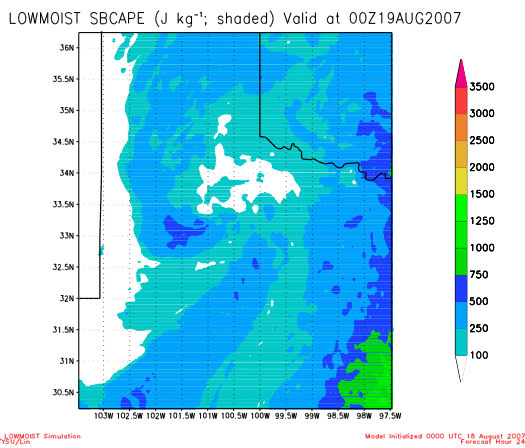
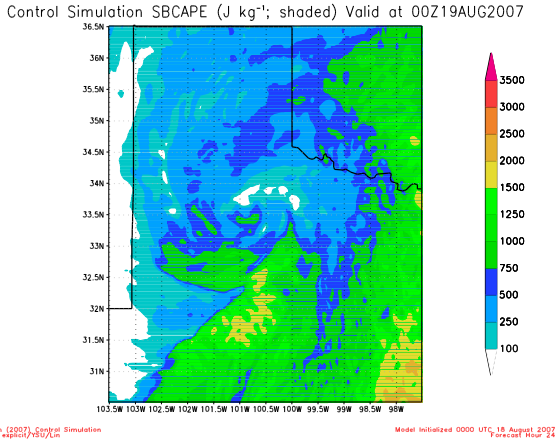


Figure 8: (a; top) Cyclone-centered surface-based CAPE from the control simulation of TC Erin at 0000 UTC 19 August 2007. (b; bottom) As in (a), except for the LOWMOIST simulation.

vicinity of the vortex as well as in its outer environment. During the midst of the reintensification process (Figure 9b), however, these differences largely become confined to within $\pm 1^\circ$ latitude and longitude of the simulated vortex. These difference fields reflect latent heat flux values of approximately $100\text{--}125\ W\ m^{-2}$ in the reintensifying composite and $25\text{--}50\ W\ m^{-2}$ in the non-reintensifying composite at both times in Figure 9 (not shown). This is well below ($>75\%$ lower) both the observed and simulated latent heat flux values during the daytime over land (not shown) as well as those observed at all times over the open waters within mature TCs (e.g. Cione et al. 2000, their Figure 7). It is thus an open question as to whether

latent heat fluxes on the order of $50\text{--}100\ W\ m^{-2}$ can result in the TC-like intensification shown here.

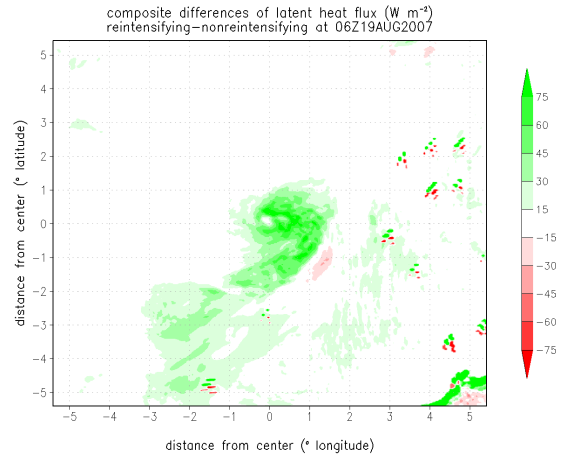
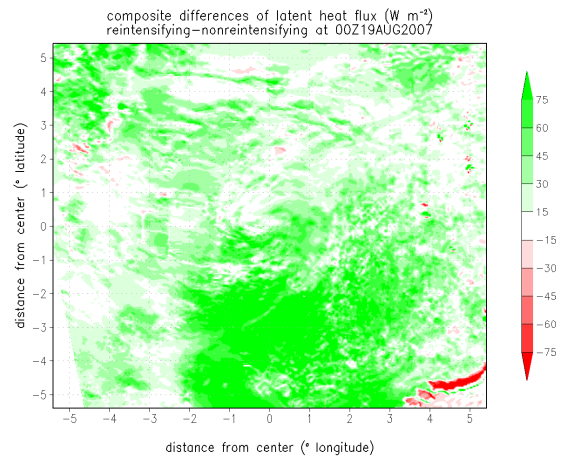


Figure 9: (a; top) As in Figure 6, except for latent heat flux ($W\ m^{-2}$). (b; bottom) As in (a), except at 0600 UTC 19 August 2007.

Two questions naturally arise from these findings. First, how do the different soil moisture initializations lead to the simulated differences in the boundary layer thermodynamic structure (e.g. as in Figure 6-9)? We believe that drier soil moisture conditions lead to greater mixing within the boundary layer, as highlighted in Figure 10. This enhanced mixing directly results in a drier, less unstable thermodynamic environment within the boundary layer both in the vicinity of the vortex (not shown) as well as in its outer environment (Figure 10). Secondly, how do these differences play a role in modulating the

intensity differences shown in Figure 5? Specifically, is the reintensification of the remnant TC Erin vortex a process that occurs as a result of enhanced latent heat fluxes underneath the cyclone (Emanuel et al. 2008), or is it a process that is modulated by the effects of drier and wetter soil conditions on the convective/thermodynamic environment surrounding the vortex during its reintensification period?

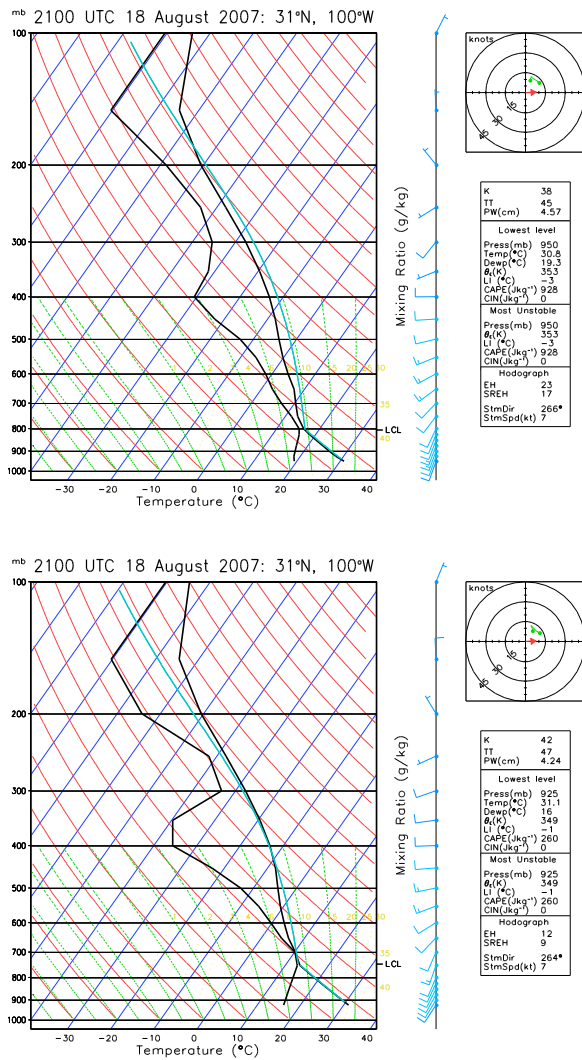


Figure 10: (a; top) Skew-T diagram at 2100 UTC 18 August 2007 at a point over southern Texas well-removed from the simulated vortex in the control simulation. (b; bottom) as in (a), except from the LOWMOIST simulation.

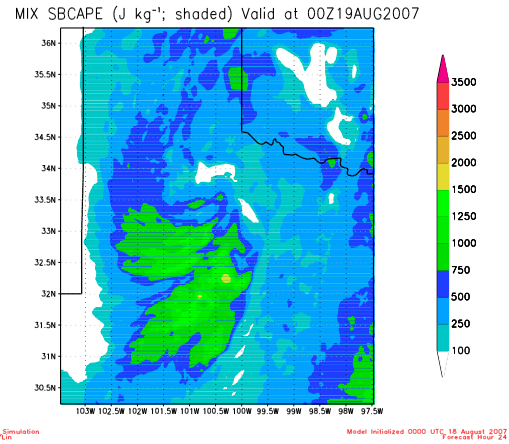


Figure 11: As in Figure 8, except for the MIX simulation.

To attempt to answer these questions, we start by comparing the control simulation to the MIX ensemble member. As stated in Section 2, this ensemble member features August 2007 soil moisture conditions along and within 1-2° of the simulated cyclone’s path and dry conditions elsewhere (Figure 4). As stated above, however, it is also among the five ensemble members that contribute to the non-reintensifying composite. More specifically, the vortex in the MIX ensemble member exhibits a pressure fall of approximately 4 hPa/12 hr, slightly higher than the non-reintensifying composite mean but also approximately half of that exhibited in the reintensifying composite mean. The boundary layer thermodynamic environment in this simulation during the early morning hours of 19 August 2007 closely resembles that of the non-reintensifying composite to the east of the vortex (c.f. Figure 11 to Figure 8b) while it more closely resembles that of the reintensifying composite near and immediately to the south of the vortex (c.f. Figure 11 to Figure 8a). Trajectory analyses from the control simulation (Figure 12) suggest that the predominant source region for parcels in the vicinity of the simulated vortex during the reintensification period is the Rio Grande Valley and western Gulf of Mexico, or along the axis of the cyclone-influenced lower tropospheric jet (not shown), rather than the region to the south and west of the vortex. This implies that the significant drying and stabilizing of the air parcels that occurs over the

artificially drier soils of southern and central Texas in the non-reintensifying simulations prohibits the vortex from reintensifying due to the impacts on the environment in which deep convection develops throughout the reintensification period. While both mechanisms are believed to be important given the evolution of the vortex within this simulation, these results suggest that the balance favors the contribution of the outer environment over that of the near-vortex environment.

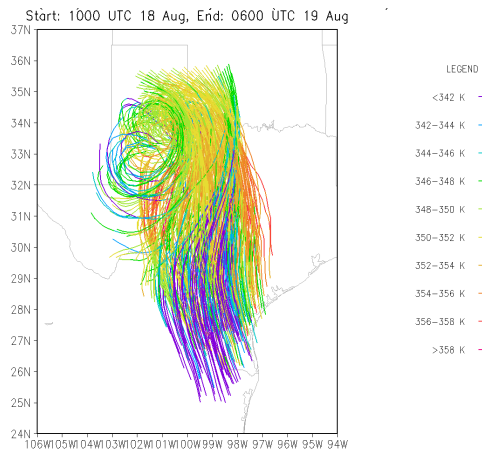


Figure 12: Back trajectory analysis starting at 0600 UTC 19 August 2007 and ending at 1000 UTC 18 August 2007 from the control simulation. Shaded is the value of equivalent potential temperature along the trajectory.

We continue to explore this issue by analyzing the output from the secondary set of ensemble simulations, the land-surface simulation members. Only one of these seven ensemble members captured the reintensification of the remnant vortex to the same magnitude as in the reintensifying composite. This ensemble member, termed LSM1, was obtained by turning off the latent heat fluxes in active areas of precipitation (i.e. underneath the vortex) starting at 0000 UTC 19 August 2007. Simulations in which the latent heat fluxes were turned off in such areas prior to this time as well as in which the latent heat fluxes were turned off everywhere at or prior to this time exhibited various degrees of pressure falls ranging from 1-5 hPa/12 hr, but none were able to capture the full

reintensification of the vortex. In general, simulations in which the latent heat fluxes were zeroed out later in the model integration, i.e. as day shifted to night on 18 August 2007, came closer to reproducing the observed reintensification than did those where the latent heat fluxes were zeroed out at or before peak heating. Turning off latent heat fluxes over part or all of the simulation domain during peak heating acts in much the same manner on the environment as do drier soil conditions; boundary layer mixing is enhanced and the thermodynamic environment becomes less unstable (not shown).

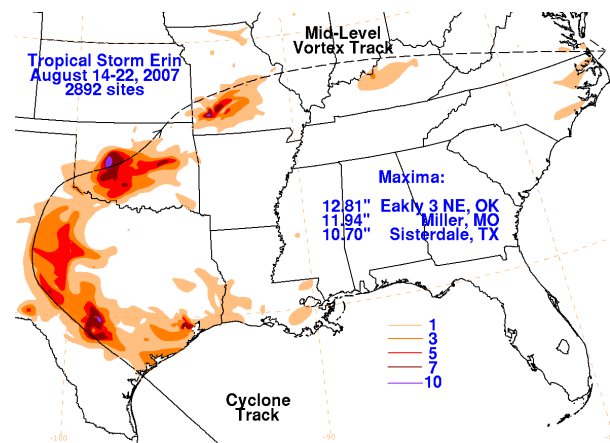


Figure 13: Observed track and rainfall totals from 14-22 August 2007 from TC Erin. Image obtained from <http://www.hpc.ncep.noaa.gov/tropical/rain/tcrainfall.html>.

The results from the ensemble of simulations of TC Erin (2007) strongly suggest that the moist, unstable environment that the remnant vortex encountered played a significant role in allowing for the observed reintensification, akin to the hypothesis of Arndt et al. (2009). This role is a multifaceted one with impacts in both the inner core of the vortex, akin to the Emanuel et al. (2008) hypothesis, as well as in its outer environment. It is the evolution in the outer environment across the southern Plains that plays the largest role in modulating the reintensification process, however. Moist, unstable parcels of air from the western Gulf of Mexico are advected inland by the cyclone-aided lower tropospheric jet, particularly at night, and maintained against mixing processes, particularly at day, by a combination of antecedently

wet soils and soils enhanced by significant rains due to TC Erin on 16-17 August 2007 (Figure 13). In the next section, we examine how these characteristics directly contribute to the reintensification of the remnant TC Erin vortex.

3.2 Physics and dynamics of the reintensification

In Section 3.1, we showed significant differences in the near-surface thermodynamic environment of the simulated cyclone between the ensemble members that captured the reintensification and those that did not. These differences lead to significant differences in the intensity of the simulated convection near and to the south and east of the simulated vortex, as captured by the area-integrated (inside 100 km radius from the center of the remnant TC Erin vortex) 600 hPa convective mass flux (Figure 14). A 25-35% greater convective mass flux, driven by stronger vertical (rising) motion in the atmospheric column, is noted with the reintensifying cases as compared to the non-reintensifying cases. This difference is largely believed to arise as a function of the partial amount of energy from the total CAPE that is actually accessed by the updrafts.

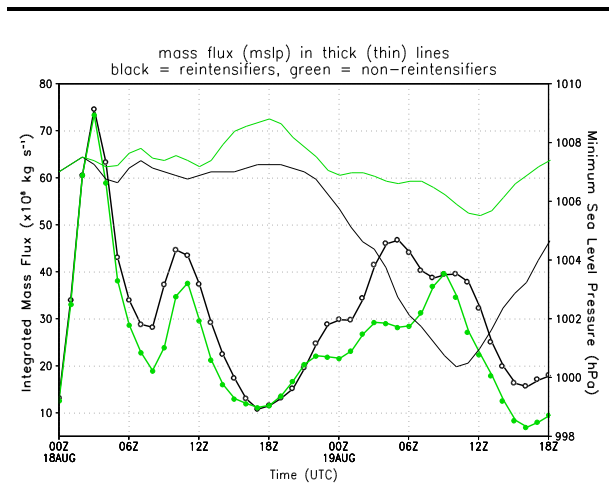


Figure 14: Composite fields of the area-integrated 600 hPa convective mass flux ($\times 10^8 \text{ kg s}^{-1}$, dotted lines) and mean sea level pressure (hPa, solid lines) between 0000 UTC 18 August 2007 and 1800 UTC 19 August 2007.

With stronger, more robust convection in the vicinity of the simulated cyclone, a greater amount of latent heat release aloft is observed with the reintensifying cases as compared to the non-reintensifying cases. This is manifest in the vertical structure of the area-averaged (inside 100 km radius) moist static energy (MSE), as depicted in Figure 15. This latent heat release aloft results in the observed pressure falls at the surface and compares favorably to the hypothesis of Arndt et al. (2009) as well as to the evolution of an intense continental mesoscale convective vortex detailed by Davis and Galarneau (2009). The convective elements in the rain band immediately east of the simulated vortex that contribute to this evolution of the MSE field have a structure similar to that exhibited with both TC rain bands found offshore (Hence and Houze 2008) as well as those found with landfalling TCs (e.g. Eastin and Link 2009), though further work is necessary to quantify such similarities.

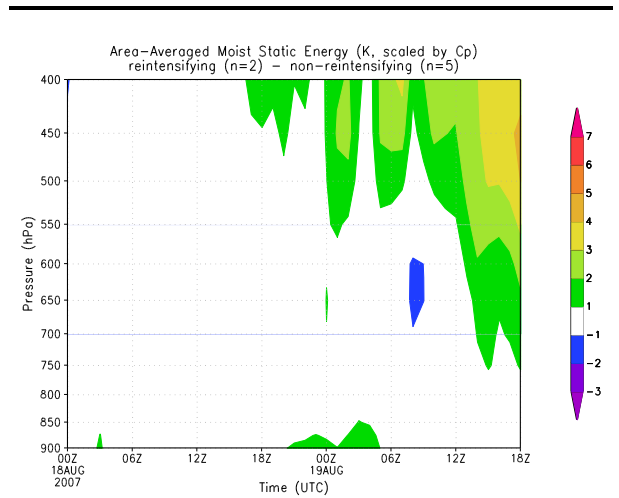


Figure 15: Composite difference (reintensifying minus non-reintensifying) of the area-averaged 900-400 hPa moist static energy (K, scaled by C_p) between 0000 UTC 18 August 2007 and 1800 UTC 19 August 2008.

We now turn to how the reintensification as a whole is manifest through a dynamical perspective. Figure 16 depicts the area-integrated (inside 100 km) lowest model level convergence from the reintensifying and non-reintensifying composite cases.

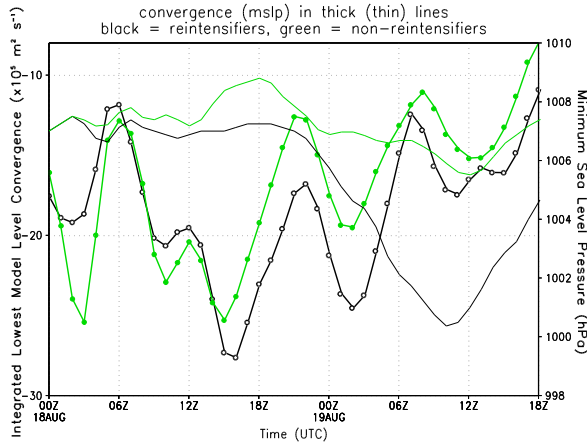


Figure 16: As in Figure 14, except for area-integrated lowest model level convergence ($\times 10^5 \text{ m}^2 \text{ s}^{-1}$, dotted lines).

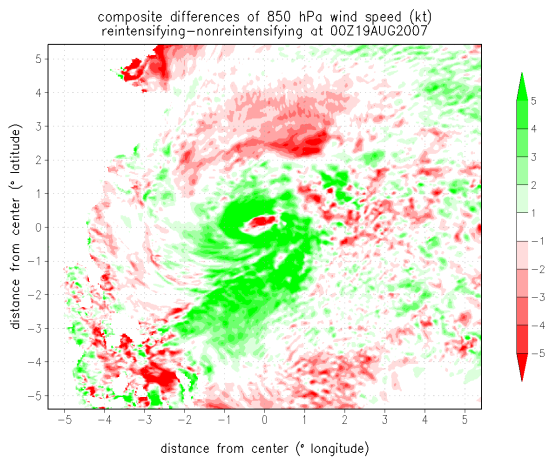


Figure 17: As in Figure 6, except for 850 hPa wind speed (kt).

Prior to and throughout the reintensification period, 10-20 % greater convergence is noted near the remnant vortex. While some of this may be due in part to a stronger vortex in and of itself, the fact that this composite difference is largely maintained through time despite the evolution of the vortex suggests a significant contribution to this evolution from external/environmental factors. We hypothesize that this difference arises primarily due to differences in the structure and intensity of the lower tropospheric jet immediately to the east of the cyclone (Figure 17). Specifically, a stronger jet coupled with the movement

of the vortex into the nose of the jet and axis of the stronger flow results in enhanced convergence in the immediate vicinity of the vortex. This enhances the convergence of meso- α scale convectively-generated vortices from the cyclone's primary rain band near the center of the vortex (Figure 18), similar to the findings of Sippel et al. (2006) for a case of tropical cyclogenesis. Furthermore, inside of these convective elements, significant tilting and stretching occurs (Figure 19a), contributing to a significant spin-up of the vortex in the boundary layer (Figure 19b) and, presumably, at the surface. The magnitude of this effect is 25-35 % greater within the reintensifying composite as compared to the non-reintensifying composite, suggesting again that the strength of the lower tropospheric convergence associated with the lower tropospheric jet and the vigor of the convection modulated by the thermodynamic environment across the southern Plains are the key factors modulating the reintensification process. Preliminary results using the circulation budget analysis of Davis and Galarneau (2009) to further quantify this evolution verify the importance of stretching and tilting processes in modulating the evolution of the vortex's circulation (not shown).

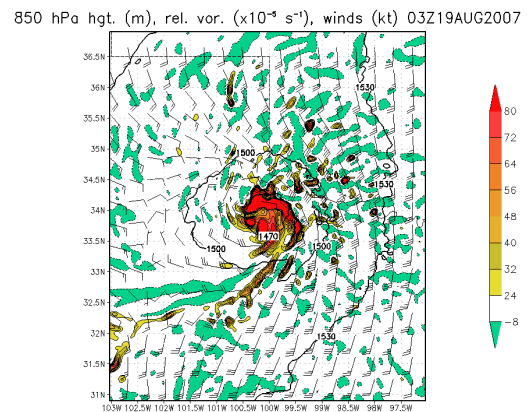


Figure 18: Cyclone-centered plot of 850 hPa relative vorticity (shaded, $\times 10^5 \text{ s}^{-1}$), winds (barbs, kt), and heights (contoured, m) at 0300 UTC 19 August 2007 from the control simulation.

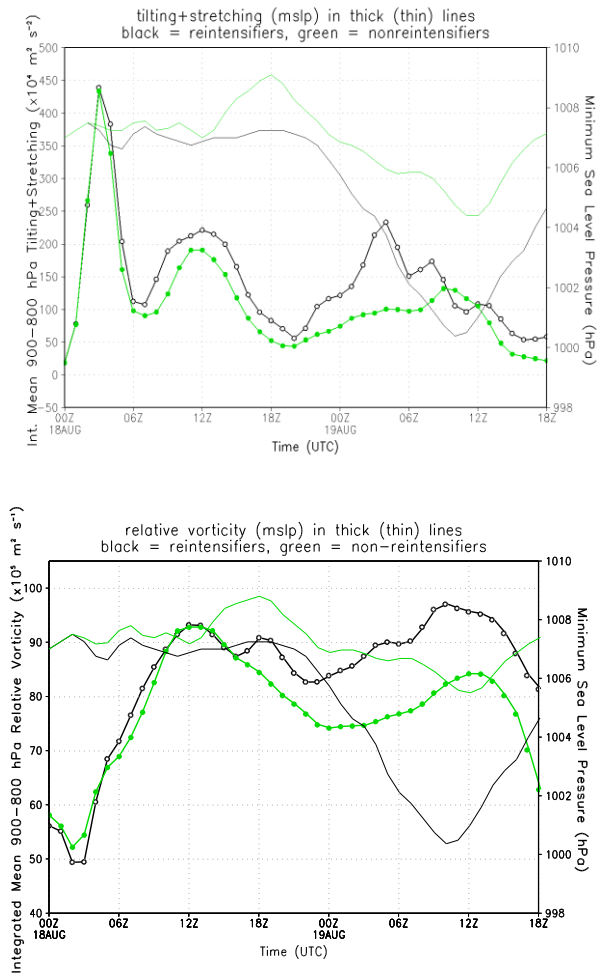


Figure 19: (a; top) As in Figure 14, except for the area-integrated mean 900-800 hPa tilting+stretching vorticity tendency ($\times 10^4 \text{ m}^2 \text{ s}^{-2}$). (b; bottom) As in (a), except for the area-integrated mean 900-800 hPa relative vorticity ($\times 10^5 \text{ m}^2 \text{ s}^{-1}$).

4. Conclusions

The dramatic overland reintensification of TC Erin (2007) is shown to largely be influenced by two factors: a moist, unstable thermodynamic environment modulated by moist soil conditions over southern and central Texas (an instability criterion) and the interaction of the remnant vortex with the cyclone-influenced nocturnal lower tropospheric jet across the southern Plains (a dynamical/lifting criterion). These two factors allow for the development of intense deep convection along a rain band to the immediate south and east of the remnant

vortex. Transport along this rain band due to the lower tropospheric jet results in convectively-generated vortices converging into the northeast quadrant of the remnant vortex, where they potentially axisymmetrize (e.g. Melander et al. 1987) about the center of circulation. Latent heat release aloft associated with the convective elements in the rain band and, ultimately, about the center of the vortex leads to intense pressure falls atop the remnant vortex. A minor influence upon the evolution is noted from latent heat fluxes at night beneath the center of circulation. A distinct lack of extratropical influence upon this evolution is observed as gauged by the Eady baroclinic growth rate and synoptic-scale quasigeostrophic forcing diagrams (not shown).

These findings best support the hypotheses of Ardnt et al. (2009) with only minor applicability of the Emanuel et al. (2008) hypothesis to this case observed. The importance of the diurnal cycle, lower tropospheric jet, and convective processes argues that the evolution of TC Erin during the reintensification process is most like that of a convectively-generated mesoscale convective vortex with some elements similar to those observed with purely tropical cyclones. Furthermore, the combination of the thermodynamic and dynamic controls on the evolution, their frequency of occurrence, and regionality of both these controls and the track of the vortex suggest that the reintensification of a TC over land in a fashion similar to TC Erin (2007) is likely to be extremely rare. Ongoing work is aimed at quantifying the degree of rarity of this evolution.

Many unanswered questions still exist regarding the evolution of TC Erin (2007). First, why did the vortex reintensify during the early morning hours of 19 August 2007 and not during the early morning hours of 18 August 2007 under similar ambient conditions? We hypothesize that the movement of the remnant vortex into, rather than along, the lower tropospheric jet axis is critical to this evolution. Secondly, how critical is the structure of the vortex, whether over water before landfall or immediately prior to the reintensification, to the ability of it to reintensify on 19 August? Similarly, how

critical is the structure of the lower tropospheric jet on 19 August 2007 to the reintensification of the vortex? Future work is aimed at answering these last two questions by considering an idealized perspective of a vortex interacting with a lower tropospheric jet.

Acknowledgments

We gratefully acknowledge insightful discussions on this work with Lance Bosart (SUNY, Univ. at Albany), George Bryan, Chris Davis, Ethan Gutmann, and Morris Weisman (all NCAR), Chuck Doswell, Michael French (Univ. of Oklahoma), Eric Hendricks (NRL-Monterey), and Paul Reasor (NOAA/AOML/HRD). Radar data depicted in Figure 1 were obtained from the National Climatic Data Center and displayed using the GRLevel2 radar viewer. Supercomputing resources for this work were provided by the NCAR bluefire and the Florida State University High Performance Computing supercomputing facilities. The third author was partially supported by NSF Grant No. ATM-0553017. NCAR is sponsored by the National Science Foundation.

References

Arndt, D. S. and coauthors, 2009: Observations of the overland reintensification of Tropical Storm Erin (2007). *Bull. Amer. Meteor. Soc.*, **90**, 1079-1093.

Bassill, N. P., and M. C. Morgan, 2006: The overland reintensification of Tropical Storm Danny (1997). Preprints, *27th Conf. on Hurricanes and Tropical Meteorology*, Monterey, CA, Amer. Meteor. Soc., 6A.6. [Available online at <http://ams.confex.com/ams/pdfpapers/108676.pdf>.]

Bosart, L. F., and G. M. Lackmann, 1995: Post-landfall tropical cyclone reintensification in a weakly baroclinic environment: A case study of Hurricane David (September 1979). *Mon. Wea. Rev.*, **123**, 3268–3291.

Brennan, M. J., R. D. Knabb, M. Mainelli, and T. B. Kimberlain, 2009: Atlantic hurricane season of 2007. *Mon. Wea. Rev.*, **137**, 4061-4088.

Chang, H.-I. and coauthors, 2009: Possible relation between land surface feedback and the post-landfall structure of monsoon depressions. *Geophys. Res. Lett.*, **36**, L15286.

Cione, J. J., P. G. Black, and S. H. Houston, 2000: Surface observations in the hurricane environment. *Mon. Wea. Rev.*, **128**, 1550-1561.

Davis, C. A. and T. J. Galarneau, 2009: The vertical structure of mesoscale convective vortices. *J. Atmos. Sci.*, **66**, 686-704.

Eastin, M. D. and M. C. Link, 2009: Miniature supercells in an offshore outer rainband of Hurricane Ivan (2004). *Mon. Wea. Rev.*, **137**, 2081-2104.

Emanuel, K. A., 1986: An air–sea interaction theory for tropical cyclones. Part I: Steady-state maintenance. *J. Atmos. Sci.*, **43**, 585–605.

Emanuel, K. E., 2008: Non-baroclinic inland rejuvenation of tropical cyclones. *Presentation given at the 14th Cyclone Workshop*, 22-26 September 2008, Sainte-Adele, Quebec, Canada.

Emanuel, K. A., J. Callaghan, and P. Otto, 2008: A hypothesis for the re-development of warm-core cyclones over northern Australia. *Mon. Wea. Rev.*, **136**, 3863-3872.

Hence, D. A. and R. A. Houze, 2008: Kinematic structure of convective-scale elements in the rainbands of Hurricanes Katrina and Rita (2005). *J. Geophys. Res.*, **113**, D15108.

Koster, R. D. and coauthors, 2009: On the nature of soil moisture in land surface models. *J. Climate*, **22**, 4322-4335.

Melander, M. V., J. C. McWilliams, and N. J. Zabusky, 1987: Axisymmetrization and vorticity-gradient intensification of an isolated two-dimensional vortex through filamentation. *J. Fluid Mech.*, **178**, 137-159.

Shen, W., I. Ginis, and R. E. Tuleya, 2002: A numerical investigation of land surface water on landfalling hurricanes. *J. Atmos. Sci.*, **59**, 789-802.

Sippel, J. A., J. W. Nielsen-Gammon, and S. E. Allen, 2006: The multiple-vortex nature of tropical cyclogenesis. *Mon. Wea. Rev.*, **134**, 1796-1814.

Skamarock, W. C. and coauthors, 2008: A description of the Advanced Research WRF version 3. NCAR Technical Note NCAR/TN-475+STR, 125pp.

Tuleya, R. E., 1994: Tropical storm development and decay: sensitivity to surface boundary conditions. *Mon. Wea. Rev.*, **122**, 291-304.